ACS APPLIED MATERIALS & INTERFACES

Research Article

www.acsami.org

Fabrication of Bifunctional Gold/Gelatin Hybrid Nanocomposites and Their Application

Qianling Cui,[†,‡,§] Alexey Yashchenok,[‡] Lu Zhang,[‡] Lidong Li,[*,†] Admir Masic,[‡] Gabriele Wienskol,[‡] Helmuth Möhwald,[‡] and Matias Bargheer[*,§]

[†]School of Materials Science and Engineering, University of Science and Technology Beijing, Beijing 100083, China

[‡]Max-Planck Institute of Colloids and Interfaces, Golm-Potsdam 14476, Germany

[§]Institute of Physics and Astronomy, University of Potsdam, Potsdam 14476, Germany

Supporting Information

ABSTRACT: Herein, a facile method is presented to integrate large gold nanoflowers (~80 nm) and small gold nanoparticles (2−4 nm) into a single entity, exhibiting both surface-enhanced Raman scattering (SERS) and catalytic activity. The as-prepared gold nanoflowers were coated by a gelatin layer, in which the gold precursor was adsorbed and in situ reduced into small gold nanoparticles. The thickness of the gelatin shell is controlled to less than 10 nm, ensuring that the small gold nanoparticles are still in a SERS-active range of the inner Au core. Therefore, the reaction catalyzed by these nanocomposites can be monitored in situ using label-free SERS spectroscopy. In addition, these bifunctional nanocomposites are also attractive candidates for application in SERS monitoring of bioreactions because of their excellent biocompatibility.

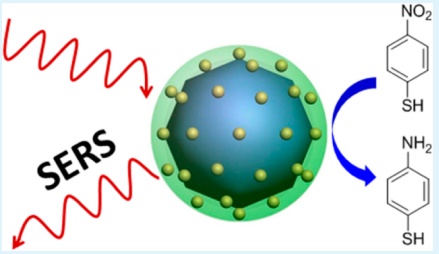

KEYWORDS: *core−shell nanostructure, gold, hybrid material, gelatin, nanoparticles, surface-enhanced Raman scattering*

INTRODUCTION

Surface-enhanced Raman scattering (SERS) is a highly sensitive technique, providing fingerprint vibrational information of molecules on a plasmonic surface for qualitative and quantitative analysis.[1] Using SERS to monitor chemical or biochemical reactions may help to better understand reaction mechanisms and kinetics.[2−4] Among them, heterogeneous catalysis with noble metal nanoparticles draws considerable interests, but the information on the reactive interfaces is still to be explored. From the different noble metal catalysts, gold nanoparticles (AuNPs) attract special attention as promising catalysts with high selectivity under mild conditions.[5]

In recent years, pioneering works have explored the fabrication of bifunctional systems combining both catalytic and SERS activity, providing new insights into the mechanism, kinetic and structural evolution of catalytic reactions by Raman spectroscopy.[2,4,6−10] One common strategy to achieve this goal is coating a SERS active core with a catalytically active surface (such as Pt, Pd),[11] and an alternative way is to assemble them into one unit.[12] In the work of Joseph et al.,[12] isolated 40 nm AuNPs and 2 nm PtNPs were deposited simultaneously onto the glass substrate, and the kinetics of Pt-catalyzed reactions were studied in detail using SERS. However, since the two kinds of metal NPs were not chemically bonded, they are not suitable for a reaction as colloidal systems under real catalytic conditions. Xie and coworkers designed and prepared raspberry-like Au/Pt/Au core−shell bimetallic nanoparticles, comprising a SERS active large Au core and a catalytically active Pt shell, where the SERS monitoring was achieved.[5] Recently, they also developed a core−satellite superstructure integrating both SERS and catalytic activity.[8] Small AuNPs were attached onto the silica-shell-isolated AuNP core through their strong affinity to thiol groups, which were modified on the silica surface. However, the present preparation methods of such bifunctional systems are quite elaborate, and finding a facile and efficient way to organize SERS and catalytically active nanoparticles into well-defined nanostructures is still a big challenge.

In this work, we design a bifunctional hybrid core-shell nanocomposite, where large AuNPs are chosen as the SERS active core, and small AuNPs with size of about 2−4 nm obtained from an in situ reduction in a 10 nm thick gelatin shell act as the catalyst (see Scheme 1). The morphology of the AuNF@Gelatin-AuNP nanocomposites obtained was characterized by transmission electron microscopy (TEM). The 4-nitrothiophenol molecule was used as a probe to examine the SERS performance of this hybrid nanocomposite. Furthermore, the whole process of the gold-catalyzed reduction of 4-nitrothiophenol by sodium borohydride was recorded by in situ SERS spectroscopy.

EXPERIMENTAL SECTION

Materials. Chloroauric acid tetrahydrate ($HAuCl_4{\cdot}4H_2O$), 4-nitrothiophenol (4-NTP), glutaraldehyde, sodium borohydride

Received: November 11, 2013
Accepted: January 9, 2014
Published: January 9, 2014

   dx.doi.org/10.1021/am5000068 | ACS Appl. Mater. Interfaces 2014, 6, 1999−2002

Scheme 1. Schematic Illustration of the Synthesis Route of Bifunctional AuNF@Gelatin−AuNP Nanocomposites

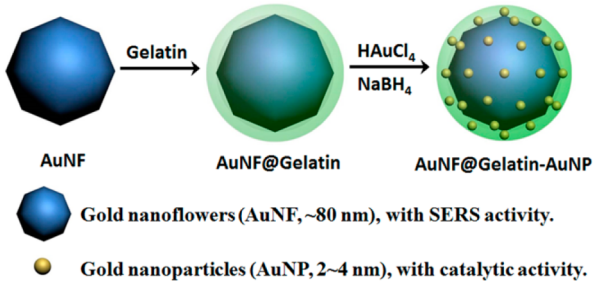

($NaBH_4$), hydrochloric acid (HCl), gelatin from cold water fish skin and 2-[4-(2-hydroxyethyl)-1-piperazinyl]ethanesulfonic acid (HEPES) were purchased from Sigma-Aldrich. All chemical reagents were used as received without further purification. Ultrapure Millipore water (18.6 MΩ) was used throughout the experiments.

Synthesis of AuNF@Gelatin-AuNP Nanocomposites. Gold nanoflowers (AuNFs) were prepared as described previously.[13,14] Briefly, 200 μL of 100 mM HEPES (pH 7.4 ± 0.5) were mixed with 1.8 mL of deionized water, followed by addition of 40 μL of 25 mM $HAuCl_4$ solution. The resultant solution was mixed by gentle inversion and left undisturbed at room temperature for 2 h.

Twenty-five milligrams of gelatin was dissolved in 8 mL of H_2O at 50 °C, and 2 mL of AuNF solution were then added under vigorous stirring. This mixture was stirred at 50 °C for 30 min, after which its pH was adjusted to ~3.0 using 1 M HCl. Then under constant stirring at 40 °C, 30 mL of acetone were added dropwise during 15 min. Seventy microliters of 25% glutaraldehyde was admixed to the stirring mixture, which was further stirred at 40 °C for 1 h, followed by overnight incubation at room temperature. The AuNF@Gelatin NPs were then collected by centrifugation, washed with water twice, and finally dispersed in H_2O.

For the formation of small gold nanoparticles (AuNPs), 30 μL of 25 mM $HAuCl_4$ solution was added into the dispersion of AuNF@Gelatin NPs and incubated at room temperature for 30 min. After centrifugation to remove the excess gold precursor, 200 μL of 10 mM $NaBH_4$ solution was added quickly to the mixture under vigorous stirring. The AuNF@Gelatin−AuNP nanocomposites were then collected by centrifugation and dispersed in H_2O.

In Situ Monitoring of the Catalytic Reaction with SERS. Ten microliters of 10 mM 4-NTP ethanol solution was added to 1 mL of colloidal suspension of AuNF@Gelatin-AuNP nanocomposites. To remove the free 4-NTP molecules, we washed the nanocomposites with water and resuspended in 500 μL of H_2O. One-hundred microliters of 20 mM $NaBH_4$ solution were added to this mixture to start the catalytic reaction. SERS spectra were collected directly from the colloidal suspension at different reaction times.

Characterization. TEM images were obtained with a Zeiss EM 912 Omega transmission electron microscope operated at 120 kV, for which samples were placed onto the carbon-coated copper grids. The Raman spectra were obtained using a confocal Raman microscope (alpha 300, WITec, Ulm, Germany) equipped with He−Ne laser excitation at a wavelength of 633 nm. The laser beam was focused through a 60× water immersion (Nikon, NA = 1.0) microscope objective. The spectra were acquired with a thermoelectrically cooled CCD detector (DU401A-BV, Andor, UK) placed behind the spectrometer (UHTS 300; WITec, ULM, Germany) with a spectral resolution of 3 cm^{-1}.

RESULTS AND DISCUSSION

The synthesis route of AuNF@Gelatin−AuNP nanocomposites is depicted in Scheme 1. Gold nanoflowers (AuNFs) with diameter of ~80 nm were used as the core, since gold nanoparticles with sizes around 60−80 nm were reported to exhibit the highest SERS efficiency.[15] The rough surface and multiple tips on it may provide many potential "hot spots", where the localized electromagnetic field is coupled and enhanced significantly. Moreover, the synthesis of AuNFs follows a simple recipe without complex experimental environment, and the relatively "clean" surface without any presence of toxic surfactant enables further modification. It is well-known that the electromagnetic field enhancement decays nearly exponentially with distance from the metal surface.[1] The gelatin shell thickness is chosen to be thin enough for high SERS efficiency and thick enough to absorb enough gold precursors which are transformed to catalytically active small AuNPs in an in situ reduction. Gelatin is a natural biomaterial which can be deposited on the AuNFs with variable thickness in the nanometer range. More importantly, there is an abundance of amino groups (from arginine and lysine) and other groups or charges on gelatin chains, offering lots of binding sites for gold ions. This maximizes the number of gold precursors and leads to a high-loading of AuNPs in the gelatin layer.

AuNFs were prepared through a simple one-step reaction under ambient temperature, using 2-[4-(2-hydroxyethyl)-1-piperazinyl]ethanesulfonic acid (HEPES) as a weak reducing and stabilizing agent.[13] Its morphology is revealed by TEM image, as shown in Figure 1A, indicating that the gold

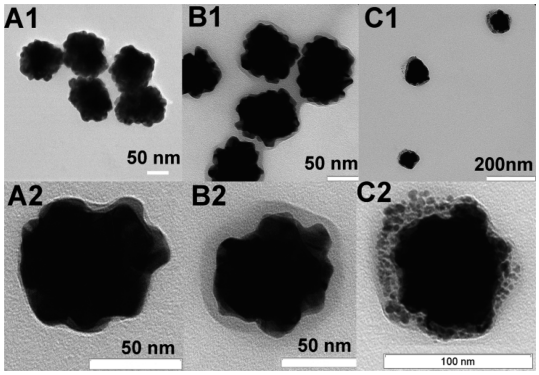

Figure 1. TEM images and magnified TEM images of the obtained AuNF (A1, A2), AuNF@Gelatin (B1, B2), and AuNF@Gelatin-AuNP (C1, C2) nanoparticles.

nanoparticles have a flower-like structure with average size around 80 nm. Next, one thin layer of gelatin shell was deposited on the AuNF surface through a temperature induced sol-gel phase transition, whose thickness can be varied easily by controlling the concentration of gelatin, as demonstrated in our previous work.[14] To keep this biomacromolecular layer more stable and compact, glutaraldehyde was used to cross-link the gelatin chains. This cross-linking process is necessary since some free gelatin chains might be washed away gradually in the following washing procedures and centrifugations. Furthermore, it avoids the possible leak of small AuNPs from the gelatin shell and keeps them close to the inner Au core. The core−shell structure of AuNF@Gelatin can be seen clearly from Figure 1B, where the thickness of the gelatin layer is less than 10 nm. The gold precursor $HAuCl_4$ solution was incubated with AuNF@Gelatin NPs until the adsorption equilibrium was reached, and the free gold ions in bulk solution were removed by subsequent centrifugation. Once the fresh $NaBH_4$ solution was added as a strong reducing agent, small AuNPs were formed in the gelatin shell. From Figure 1C it can be seen that a number of small AuNPs with sizes between 2 and 4 nm surround the large AuNF core. These small AuNPs

get close enough to the SERS-active core to support the bifunctional behavior of the unit, as will be shown below.

The plasmon resonance band of AuNFs in aqueous solution located around 600 nm, is shifted about 18 nm towards longer wavelength after coating with a gelatin layer. This red-shift can be explained by the increase in the local refractive index of the surrounding medium,[16] which changes from water (1.33) to gelatin (1.53). When the small AuNPs were introduced into the gelatin layer, the effective dielectric constant of the shell around the AuNF core further increased,[16] leading to another 10 nm red-shift in the extinction spectra of AuNF@Gelatin-AuNP nanocomposites (see the Figure S1 in the Supporting Information). This moves the plasmon resonance close to the excitation wavelength (633 nm) for Raman spectroscopy, which is favorable to get large enhancement of electromagnetic field and Raman signal.

Small AuNPs with diameter less than 10 nm are mild catalysts, which are suitable for a slow catalytic reaction at ambient temperature. The catalytic reduction of nitroaromatic molecule to its corresponding aniline derivative is utilized here as a model reaction to examine the performance of the hybrid nanocomposite with catalytic activity of the 2−4 nm particles embedded in the gelatin shell.

First, we confirm the enhancement of the Raman scattering induced by the AuNF. The Raman spectra were obtained using a confocal Raman microscope equipped with He−Ne laser excitation at a wavelength of 633 nm. Throughout each figure, the conditions for obtaining Raman signals are kept constant. Figure 2A compares the spectrum of solid 4-nitrothiophenol

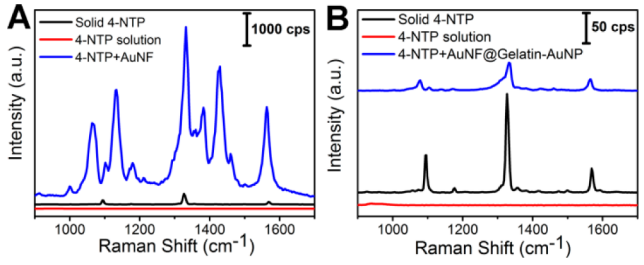

Figure 2. (A) Raman spectra of solid 4-NTP (black curve), 4-NTP solution (red curve), and SERS spectra of 4-NTP enhanced by bare AuNFs (blue curve). (B) Raman spectra of solid 4-NTP (black curve), 4-NTP solution (red curve), and SERS spectra of 4-NTP enhanced by AuNF@Gelatin−AuNP nanocomposites (blue curve). The concentration of 4-NTP in the solution is 1×10^{-4} M. The spectra are offset vertically for clarity.

(4-NTP) to the strongly surface enhanced spectrum of a 4-NTP solution on bare AuNFs. The characteristic symmetric NO_2 stretching at 1327 cm^{-1} and the C═C stretching of the phenyl ring at 1568 cm^{-1} identify the reactant. In the bare AuNF sample, the C−H bending on the phenyl ring modes at 1172 and 1096 cm^{-1} (see also Figure 2B) are covered by a nearby band at 1132 cm^{-1} of an unwanted product of the dimerization reaction of 4-NTP towards 4,4′-dimercaptoazobenzene (DMAB), which is identified by the strong new bands at 1381 and 1429 cm^{-1}. For comparison, the red lines in A and B in Figure 2 confirm that the Raman signal of 4-NTP solution at the same concentration (1×10^{-4} M); however, in absence of AuNPs, is well below the detection threshold. Binding 4-NTP to the bare AuNF surface enhances its Raman signal by 6 orders of magnitude (blue curve in Figure 2A). This photocatalytic side reaction to DMAB was also observed in previous studies, where the 4-NTP was directly exposed to the metal surface with strong SERS activity under laser irradiation.[7,17−19] Xie et al. used a thin silica shell on the inner Au core to prevent direct contact of the 4-NTP molecules with the SERS active Au surface.[8] Figure 2B shows that in our experiment, the presence of a thin gelatin layer also eliminates the unwanted photocatalytic side reaction, as the vibration bands of DMAB essentially vanish. We use the enhancements to NO_2 vibration to estimate the enhancement factor, according to calculation method in literatures.[20,21] The enhancement factors for AuNFs and AuNF@Gelatin−AuNP were estimated to be 1.6×10^6 and 2.8×10^4, respectively. It can be concluded that gelatin shell reduces the Raman enhancement of 4-NTP by about 50-fold in comparison to that on bare AuNFs. However, the SERS signal intensity in the AuNF@Gelatin-AuNP composite at low concentration remains comparable to bulk 4-NTP, i.e., strong enough to be used as an analytical tool.

To demonstrate the hybrid nature of the AuNF@Gelatin−AuNP nanocomposites, we loaded the colloidal solution with 4-NTP molecules and triggered the reaction from 4-NTP to 4-aminothiophenol (4-ATP), catalyzed by the small AuNP embedded in the gelatin shell, by adding a small amount of $NaBH_4$ aqueous solution. Figure 3A shows a sequence of SERS

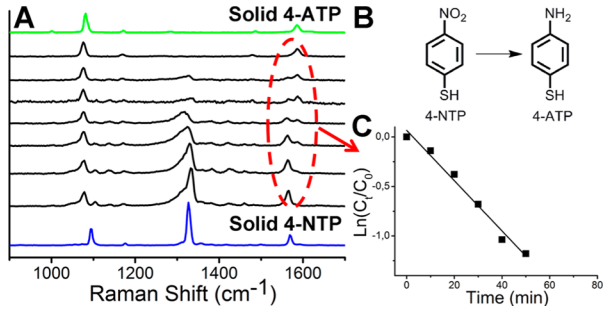

Figure 3. (A) SERS spectra recorded during the reduction of 4-NTP in AuNF@Gelatin−AuNP nanocomposites at different reaction times. From bottom to top: SERS spectra recorded at 0, 10, 20, 30, 40, 50, and 90 min after addition of $NaBH_4$ solution. The blue curves are the Raman spectra of solid 4-NTP and 4-ATP. The spectra are offset vertically for clarity. (B) Chemical structures of 4-NTP reactant and 4-ATP product. (C) Plot of $\ln(C_t/C_0)$ of 4-NTP as a function of time for the reaction catalyzed by AuNF@Gelatin−AuNP nanocomposites.

spectra indicating a gradual decrease of the NO_2 stretching band at 1327 cm^{-1} on a 30 min time scale. The band disappeared after 90 min, indicating that the nitro groups on 4-NTP were catalytically reduced completely. The band at 1568 cm^{-1} ascribed to the phenyl ring modes of 4-NTP decreases gradually, accompanied by a new peak at 1588 cm^{-1}, which is assigned to the 4-ATP product. The shift of the C═C vibration in the phenyl ring from 1568 to 1588 cm^{-1} is an excellent fingerprint of a reaction from 4-NTP to 4-ATP as the oscillator strength remains approximately constant, and thus also the formation of the product can be observed. By comparing the intensities of the two characteristic bands, the relative concentration of 4-NTP and 4-ATP is calculated quantitatively. Figure 3C shows the plot of $\ln(C_t/C_0)$ as a function of reaction time, where C_t and C_0 are the relative concentrations of 4-NTP at time t and 0, respectively. The linear relationship indicates that this catalytic reaction follows a pseudo-first-order kinetics, because of its independence on the concentration of $NaBH_4$, which was in large excess compared to 4-NTP. The Raman

dx.doi.org/10.1021/am5000068 | ACS Appl. Mater. Interfaces 2014, 6, 1999−2002

spectrum of the final product after the completion of the reduction is consistent with that of 4-ATP reported in literature.[17]

To confirm the bifunctional nature of our AuNF@Gelatin−AuNP nanocomposites, we confirmed that the 4-NTP molecules were preferentially catalyzed by the small AuNPs, which were embedded in the gelatin shell that prevents the side reaction to DMAB: The reaction shown in Figure 3 was monitored once more using UV−vis absorption spectroscopy, as shown in Figure S2 in the Supporting Information. The initial 4-NTP solution with excess of $NaBH_4$ showed an absorption band around 410 nm, attributed to the formation of 4-nitrothiophenolate ions in alkaline condition. After addition of AuNF@Gelatin−-AuNP colloids, the absorption band decreased gradually, and the color of the mixture changed from yellow to colorless. When AuNF@Gelatin without small AuNP were added no color change was observed. This control experiment confirms that the reaction is only catalytic, i.e., not photoinduced. On the other hand, in the reaction process, it can not be completely excluded that a small portion of 4-NTP molecules perhaps reached the large core. However, the photochemical reaction was not significant, because the Raman result did not show obvious Raman bands of the side-product, 4,4′-dimercaptoazobenzene (DMAB). We also believed that the catalysis reaction indeed occurred on the small AuNP in gelatin layer, because the large AuNF itself cannot catalyze efficiently this reduction reaction as demonstrated by UV-vis absorption spectra (see Figure S2 in the Supporting Information). Although UV−vis absorption spectroscopy is widely used for monitoring this reduction reaction, it provides limited information about the structure, and it will not work if the concentration of reactant is low. In addition, SERS allows simultaneously monitoring the emerging bands of the product even at low concentration, making it a better choice, in particular because of the additional structural information encoded in multiple bands.

CONCLUSIONS

In conclusion, a facile method was presented to fabricate a bifunctional AuNF@Gelatin-AuNP nanocomposite, consisting of a large AuNF core with SERS ability and small AuNPs in a gelatin shell with catalytic activity. Since the thickness of the gelatin shell is less than 10 nm, the small AuNPs embedded in it are still in the SERS active range of the AuNF core. Although the Raman enhancement of the nanocomposite was reduced about 50-fold compared to bare AuNFs due to the presence of the gelatin layer, the Raman intensity was still strong enough to derive information on a reaction, the reduction of 4-NTP catalyzed by the nanocomposite. The photo-catalyzed dimerization of 4-NTP to DMAB was avoided to a large amount, which had previously partly interfered in SERS monitoring using bare plasmonic nanostructures. This reaction is well-studied, and we did not add new information, but the system and proceeding described in this paper are well-suited for broader application.

ASSOCIATED CONTENT

Supporting Information

Extinction spectra, absorption spectra during the catalytic reaction, estimation of Raman enhancement factor, comparison of SERS ability of AuNFs and AuNPs. This material is available free of charge via the Internet at http://pubs.acs.org.

AUTHOR INFORMATION

Corresponding Authors

*E-mail: bargheer@uni-potsdam.de.
*E-mail: lidong@mater.ustb.edu.cn.

Notes

The authors declare no competing financial interest.

ACKNOWLEDGMENTS

Y.A. thanks the Alexander von Humboldt-Stiftung for the scholarship.

REFERENCES

(1) Dieringer, J. A.; McFarland, A. D.; Shah, N. C.; Stuart, D. A.; Whitney, A. V.; Yonzon, C. R.; Young, M. A.; Zhang, X. Y.; Van Duyne, R. P. *Faraday Discuss.* **2006**, *132*, 9−26.
(2) Heck, K. N.; Janesko, B. G.; Scuseria, G. E.; Halas, N. J.; Wong, M. S. *J. Am. Chem. Soc.* **2008**, *130*, 16592−16600.
(3) Lantman, E. M. V.; Deckert-Gaudig, T.; Mank, A. J. G.; Deckert, V.; Weckhuysen, B. M. *Nat. Nanotechnol.* **2012**, *7*, 583−586.
(4) Guerrini, L.; Lopez-Tobar, E.; Garcia-Ramos, J. V.; Domingo, C.; Sanchez-Cortes, S. *Chem. Commun.* **2011**, *47*, 3174−3176.
(5) Min, B. K.; Friend, C. M. *Chem. Rev.* **2007**, *107*, 2709−2724.
(6) Wang, A.; Huang, Y. F.; Sur, U. K.; Wu, D. Y.; Ren, B.; Rondinini, S.; Amatore, C.; Tian, Z. Q. *J. Am. Chem. Soc.* **2010**, *132*, 9534−9536.
(7) Xie, W.; Herrmann, C.; Kompe, K.; Haase, M.; Schlucker, S. *J. Am. Chem. Soc.* **2011**, *133*, 19302−19305.
(8) Xie, W.; Walkenfort, B.; Schlucker, S. *J. Am. Chem. Soc.* **2013**, *135*, 1657−1660.
(9) Ren, X. Q.; Tan, E. Z.; Lang, X. F.; You, T. T.; Jiang, L.; Zhang, H. Y.; Yin, P. G.; Guo, L. *Phys. Chem. Chem. Phys.* **2013**, *15*, 14196−14201.
(10) Muralidharan, R.; McIntosh, M.; Li, X. *Phys. Chem. Chem. Phys.* **2013**, *15*, 9716−9725.
(11) Tian, Z. Q.; Ren, B.; Li, J. F.; Yang, Z. L. *Chem. Commun.* **2007**, 3514−3534.
(12) Joseph, V.; Engelbrekt, C.; Zhang, J. D.; Gernert, U.; Ulstrup, J.; Kneipp, J. *Angew. Chem., Int. Ed.* **2012**, *51*, 7592−7596.
(13) Xie, J. P.; Zhang, Q. B.; Lee, J. Y.; Wang, D. I. C. *ACS Nano* **2008**, *2*, 2473−2480.
(14) Cui, Q. L.; He, F.; Wang, X. Y.; Xia, B. H.; Li, L. D. *ACS Appl. Mater. Interfaces* **2013**, *5*, 213−219.
(15) Krug, J. T.; Wang, G. D.; Sr, E.; Nie, S. M. *J. Am. Chem. Soc.* **1999**, *121*, 9208−9214.
(16) Kiel, M.; Klotzer, M.; Mitzscherling, S.; Bargheer, M. *Langmuir* **2012**, *28*, 4800−4804.
(17) Huang, Y. F.; Zhu, H. P.; Liu, G. K.; Wu, D. Y.; Ren, B.; Tian, Z. Q. *J. Am. Chem. Soc.* **2010**, *132*, 9244−9246.
(18) Dong, B.; Fang, Y. R.; Xia, L. X.; Xu, H. X.; Sun, M. T. *J. Raman Spectrosc.* **2011**, *42*, 1205−1206.
(19) Kang, L. L.; Xu, P.; Zhang, B.; Tsai, H. H.; Han, X. J.; Wang, H. L. *Chem. Commun.* **2013**, *49*, 3389−3391.
(20) Zhang, L.; Dong, W. F.; Tang, Z. Y.; Song, J. F.; Xia, H.; Sun, H. B. *Opt. Lett.* **2010**, *35*, 3297−3299.
(21) Orendorff, C. J.; Gole, A.; Sau, T. K.; Murphy, C. J. *Anal. Chem.* **2005**, *77*, 3261−3266.